

MU ROBUSTNESS ANALYSIS OF ADAPTIVE FEEDFORWARD NOISE CANCELLING ALGORITHMS

David S. Bayard¹

Jet Propulsion Laboratory
California Institute of Technology
4800 Oak Grove Drive
Pasadena, CA 91109

Abstract

Robust control theory is applied to analyzing a class of adaptive feedforward algorithms for cancelling sinusoidal noise. This approach differs significantly from more accepted methods of adaptive analysis using Hyperstability, Lyapunov functions, etc., and has certain advantages when studying properties of robust stability. A case study is given where the structured singular value is applied to analyzing the difficult but well-known problem for adaptive noise cancellation which arises when there is a plant resonance blocking the noise cancellation path.

1 Introduction

Robust control theory is applied to analyzing a class of adaptive feedforward algorithms for cancelling sinusoidal noise. This approach is valid for an idealized (and somewhat restrictive) situation where the noise being cancelled is assumed to have the form of a sinusoidal sum, as opposed to the more typical case of a correlated random noise process. However, sinusoidal noise arises in a reasonable range of applications (e.g., rotating machines, cryocoolers, rotocraft, etc.) and the method offers intuition into robust stability which is not presently possible using more conventional methods of adaptive analysis (e.g., such as Hyperstability, and Lyapunov methods).

The robustness analysis is based on a recently derived decomposition of an adaptive algorithm with a sinusoidal regressor into the parallel connection of an LTI block and a norm-bounded LTV block. This resulting LTI/LTV decomposition leads naturally to a robustness analysis formulation where the LTI block is interpreted as the nominal control law, the LTV block is thought of as an "additive perturbation" to the LTI block, and where additional blocks can be added to represent the uncertainties in the plant, actuators, sensors, etc..

¹Mail Stop 198-326, bayard@bert2.jpl.nasa.gov, Tel: (818) 354-8208, FAX: (818) 393-3444

A case study is given to demonstrate the method on a difficult problem for which no alternative method of analysis is available, i.e., the problem of adaptive noise cancellation when there is a plant resonance blocking the noise cancellation path, and when there is multiplicative uncertainty in the plant description.

2 Harmonic Noise Suppression

2.1 Formulation

A general formulation of the harmonic suppression problem is shown in Figure 2.1. The basic problem is to suppress the harmonic disturbance signal y of the form,

$$y = \sum_{i=1}^{\ell} \beta_i \sin(\omega_i t + \theta_i) \quad (2.1)$$

by controlling an associated error signal e to zero. In a large number of applications the error takes the form,

$$e = P(p)[y - \hat{y}] \quad (2.2)$$

The filter $P(s)$ in (2.2) is a known or partially known stable transfer function which blocks the error path. Here, \hat{y} is an estimate of y which is generated as a linear combination of the elements of the regressor vector x , i.e.,

$$\hat{y} = w^T x \quad (2.3)$$

and the parameter vector w is tuned using some adaptation mechanism, such as the ones to be considered later in this paper. The adaptive controller is denoted by the operator \mathcal{H} in Figure 2.1. As shown, \mathcal{H} is an operator which maps the error e into the estimate \hat{y} , i.e.,

$$\hat{y} = \mathcal{H}[e] \quad (2.4)$$

Simply stated, the goal of the adaptive controller \mathcal{H} is to provide high gain at the disturbance frequencies in y so as to minimize the effect of y on the plant output e .

3 Adaptive Systems with Harmonic Regressors

The specific class of \mathcal{H} to be studied in this paper is shown in Figure 3.1. Here, an estimate \hat{y} of the disturbance signal y is constructed as a linear combination of the elements of the regressor vector $x(t) \in R^N$, i.e.,

Estimated Signal

$$\hat{y} = w(t)^T x(t) \quad (3.1)$$

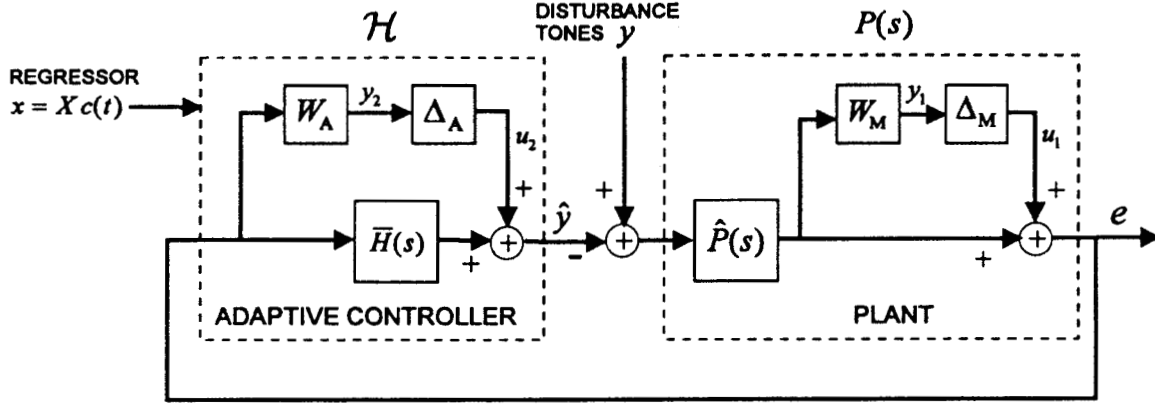


Figure 2.1: Robustness analysis of adaptive noise cancelling

where $w(t) \in R^N$ is a parameter vector which is tuned in real-time using the adaptation algorithm,

Adaptation Algorithm

$$w = \mu \Gamma(p)[\tilde{x}(t)e(t)] \quad (3.2)$$

Here, the notation $\Gamma(p)[\cdot]$ is used to denote the multivariable LTI transfer function $\Gamma(s) \cdot I$ where $\Gamma(s)$ is any LTI transfer function in the Laplace s operator (the differential operator p will replace the Laplace operator s in all time-domain filtering expressions); the term $e(t) \in R^1$ is an error signal; $\mu > 0$ is an adaptation gain; and the signal \tilde{x} is obtained by filtering the regressor x through any stable filter $F(p)$, i.e.,

Regressor Filtering

$$\tilde{x} = F(p)[x] \quad (3.3)$$

The notation $F(p)[\cdot]$ denotes the multivariable LTI transfer function $F(s) \cdot I$ with SISO filter $F(s)$, acting on the indicated vector time domain signal.

For the purposes of this paper, it will be assumed that the regressor x can be written as a linear combination of m distinct sinusoidal components $\{\omega_i\}_{i=1}^m$, $0 < \omega_1 < \omega_2 < \dots < \omega_m$, where the frequencies have been ordered by size from smallest to largest. Equivalently, it is assumed that there exists a matrix $\mathcal{X} \in R^{N \times 2m}$ such that,

Harmonic Regressor

$$x = \mathcal{X}c(t) \quad (3.4)$$

$$c(t) = [\sin(\omega_1 t), \cos(\omega_1 t), \dots, \sin(\omega_m t), \cos(\omega_m t)]^T \in R^{2m} \quad (3.5)$$

Equations (3.1)-(3.5) taken together will be referred to as a *harmonic adaptive system*. Collectively, these equations define the open-loop mapping \mathcal{H} in Figure 3.1 which will be used throughout this paper.

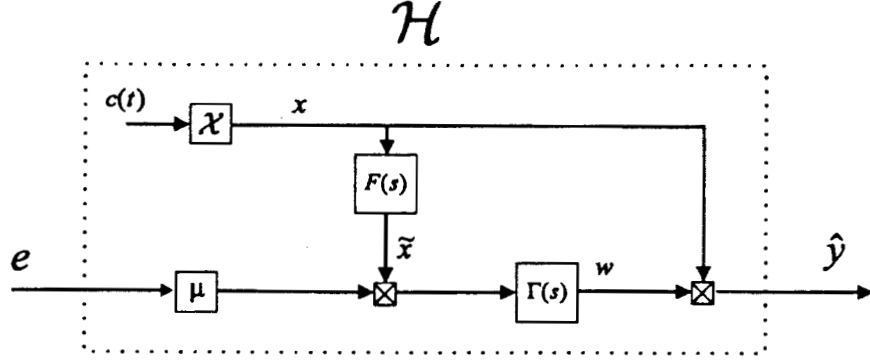


Figure 3.1: LTV operator $\hat{y} = \mathcal{H}[e]$ for adaptive system with harmonic regressor x , adaptation law $\Gamma(s)$, and regressor filter $F(s)$

3.1 LTI/LTV Decomposition

Let $D^2 \in \mathbb{R}^{2m \times 2m}$ be defined as a matrix of the pairwise diagonal form,

$$D^2 \triangleq \begin{bmatrix} d_1^2 \cdot I_{2 \times 2} & 0 & \dots & 0 \\ 0 & \ddots & \ddots & \vdots \\ \vdots & \ddots & \ddots & 0 \\ 0 & \dots & 0 & d_m^2 \cdot I_{2 \times 2} \end{bmatrix} \in \mathbb{R}^{2m \times 2m} \quad (3.6)$$

$d_i^2 \geq 0, i = 1, \dots, m, I_{2 \times 2} \in \mathbb{R}^{2 \times 2}$. Let \mathcal{X} be defined as in (3.4), and define the perturbation Δ as the deviation of $\mathcal{X}^T \mathcal{X}$ from the pairwise diagonal matrix D^2 , i.e.,

$$\Delta \triangleq \mathcal{X}^T \mathcal{X} - D^2 \quad (3.7)$$

Then it is shown in [3][1] that the mapping \mathcal{H} in Figure 3.1 can be expressed as the parallel connection of an LTI block $\bar{H}(s)$, and an LTV block $\tilde{\Delta}$, i.e.,

$$\mathcal{H}: \quad \hat{y} = \bar{H}(p)e + \tilde{\Delta}[e] \quad (3.8)$$

LTI Block

$$\bar{H}(s) \triangleq \mu \sum_{i=1}^m d_i^2 \cdot H_i(s) \quad (3.9)$$

$$H_i(s) = \frac{F_R(i)}{2} \left(\Gamma(s - j\omega_i) + \Gamma(s + j\omega_i) \right) + \frac{F_I(i)}{2j} \left(\Gamma(s - j\omega_i) - \Gamma(s + j\omega_i) \right) \quad (3.10)$$

$$F_R(i) \triangleq \text{Re}(F(j\omega_i)); \quad F_I(i) \triangleq \text{Im}(F(j\omega_i)) \quad (3.11)$$

If the adaptation law $\Gamma(s)$ is stable with infinity norm $\|\Gamma(s)\|_\infty$, then the induced 2-norm gain (denoted by $\|\cdot\|_{2i}$), of the LTV perturbation can be bounded from above as,

Bound on LTV Block

$$\|\tilde{\Delta}\|_{2i} \leq \mu m \bar{\sigma}(\Delta) \|\Gamma(s)\|_{\infty} \max_i |F(\omega_i)| \quad (3.12)$$

Remarks

As might be expected, the LTI transfer function $\bar{H}(s)$ is a function of the disturbance tone frequencies ω_i , $i = 1, \dots, m$, the regressor filter $F(s)$, the adaptive law $\Gamma(s)$, and the diagonal elements of D^2 .

Intuitively, the Δ matrix in (3.7) depicts how far away the quantity $\mathcal{X}^T \mathcal{X}$ is from some (arbitrarily specified) pairwise diagonal matrix D^2 . This in turn determines the size of the LTV perturbation in (3.12), i.e., how far away the mapping \bar{H} is from a purely LTI representation $H(s)$.

If $\mathcal{X}^T \mathcal{X} = D^2$, the “X-Orthogonality” (XO) condition is said to hold [1][2]. Under the XO condition, $\Delta = 0$ and it follows from (3.12) that the LTV block vanishes and the adaptive mapping is purely LTI. Interestingly, it has been shown in [1][2] that the XO condition is also necessary for the LTI property.

The decomposition is only unique for a specified choice of D^2 , i.e., different choices of D^2 lead to different LTI/LTV blocks in the representation. The choice of D^2 which minimizes the LTV part (in a certain bound-optimal sense), can be found by solving a related Linear Matrix Inequality (LMI) [4].

The need for $\|\Gamma(s)\|_{\infty}$ to exist in the bound (3.12) requires that the adaptive law contain a “leakage” type term to bound the adaptive gain. This is not expected to be restrictive since a small leakage term is commonly added in implementations.

If the disturbance frequencies are known, the regressor can be chosen as $x = c(t)$ where $c(t)$ has the paired sin/cos form given in (3.5). In this case $\mathcal{X} = I$ and the XO condition is satisfied by design, exactly.

In the more practical situation where the disturbance frequencies are unknown, it is difficult to satisfy the XO condition exactly. Nevertheless, it is still possible (for example by using a tap-delay line) to construct a regressor which nearly satisfies the XO condition. In this case the adaptive system is representable as an LTI block with a comparatively small LTV additive perturbation and can be conveniently analyzed as such within a modern robust control framework.

3.2 Tap-Delay Line Regressors

The theory described in previous sections is now specialized to the case where the components of the regressor $x = [x_1, \dots, x_N]^T \in R^N$ are defined by filtering a signal $\xi(t) \in R^1$ through a tap delay line with N taps and tap delay T , i.e.,

$$x_\ell = e^{-(\ell-1)pT} \xi, \quad \ell = 1, \dots, N \quad (3.13)$$

where the measured signal ξ is given by the following sum of m sinusoids,

$$\xi(t) = \sum_{i=1}^m \alpha_i \sin(\omega_i t + \phi_i); \quad \alpha_i > 0 \quad (3.14)$$

It will further be assumed that the frequencies $\{\omega_i\}_{i=1}^m$ lie in a bounded tone set $\Omega(m, T, \underline{\nu})$ defined next.

DEFINITION 3.1 *Given time delay T and spacing parameter $0 < \underline{\nu} < \pi/2$, a Bounded Tone Set $\Omega(m, T, \underline{\nu})$ is defined as any set of m frequencies $\{\omega_i\}_{i=1}^m$, such that,*

$$\Omega(m, T, \underline{\nu}) \triangleq \left\{ \begin{array}{l} \{\omega_i\}_{i=1}^m : \quad 0 < \underline{\nu} < \pi/2; \\ 0 < \underline{\nu} < \omega_i T \leq \pi - \underline{\nu} \quad \text{for all } i = 1, \dots, m; \\ |\omega_i - \omega_j| T \geq 2\underline{\nu} \quad \text{for all } i \neq j \end{array} \right\} \quad (3.15)$$

■

This definition says that the set of frequencies $\{\omega_i\}_{i=1}^m$ are bounded away from 0, π/T and each other, with *minimum spacing* parameter $\underline{\nu}$.

The TDL regressor (3.13) can be written in the standard form $x = \mathcal{X}c(t)$ (cf., [1][4]). Let D^2 be defined as follows,

$$D^2 = \frac{N}{2} \begin{bmatrix} \alpha_1^2 \cdot I_{2 \times 2} & 0 & \dots & 0 \\ 0 & \ddots & \ddots & \vdots \\ \vdots & \ddots & \ddots & 0 \\ 0 & \dots & 0 & \alpha_m^2 \cdot I_{2 \times 2} \end{bmatrix} \in R^{2m \times 2m} \quad (3.16)$$

Applying D^2 from (3.16) in the LTI/LTV decomposition (3.8) gives,

LTI/LTV Decomposition for TDL Regressor

$$\mathcal{H}: \quad \hat{y} = \overline{H}(p)e + \tilde{\Delta}[e] \quad (3.17)$$

Normalizing the adaptive gain to $\mu = \bar{\mu}/N$ in (3.9), and using (3.16) yields,

LTI Block

$$\bar{H}(s) = \frac{\bar{\mu}}{2} \sum_{i=1}^m \alpha_i^2 \cdot H_i(s) \quad (3.18)$$

where $H_i(s)$ has been defined earlier in (3.10).

Bound on LTV Block

$$\|\tilde{\Delta}\|_{2i} \leq \mu m \bar{\sigma}(\Delta) \|\Gamma(s)\|_{\infty} \max_i |F(\omega_i)| \quad (3.19)$$

In addition, the following upper bound on Δ has been proved in [1][4] in terms of the minimal spacing parameter $\underline{\nu}$,

$$\bar{\sigma}(\Delta) \leq \frac{m\pi\alpha_{max}^2}{2\underline{\nu}}; \quad \alpha_{max} \triangleq \max_i \{\alpha_i\} \quad (3.20)$$

Substituting (3.20) into (3.19) gives a useful alternative but somewhat more conservative bound,

$$\|\tilde{\Delta}\|_{2i} \leq \frac{\bar{\mu}m^2\pi}{2N\underline{\nu}} \cdot \left(\alpha_{max}^2 \|\Gamma(s)\|_{\infty} \max_i |F(\omega_i)| \right) \quad (3.21)$$

As might be expected, the bound on the LTV perturbation $\tilde{\Delta}$ in (3.21) depends on the number of taps N , the minimum spacing parameter $\underline{\nu} > 0$, the number of disturbance tones m , the disturbance tone magnitudes α_{max} , and choice of filter $F(s)$ and adaptive law $\Gamma(s)$.

According to (3.21), the size of the LTV block decays as $1/N$, and hence the system approaches a pure LTI block asymptotically as the number of taps N becomes large. This is a notable property, because in this case the regressor has been constructed without explicit knowledge of the disturbance tone frequencies beforehand. Of course this result assumes a minimum spacing between tones of $\underline{\nu}$. If this spacing decreases, it follows from (3.21) that N must be increased in proportion to $1/\underline{\nu}$ to achieve the same value for the LTV norm-bound.

For convenience, the LTI/LTV decomposition of an adaptive system having a TDL regressor is summarized in Figure 3.2. Specifically, Figure 3.2 Part a. shows the harmonic adaptive system with TDL basis and normalized adaptation gain $\mu = \bar{\mu}/N$; Part b. shows the equivalent decomposition into an LTI block and a norm bounded LTV perturbation block.

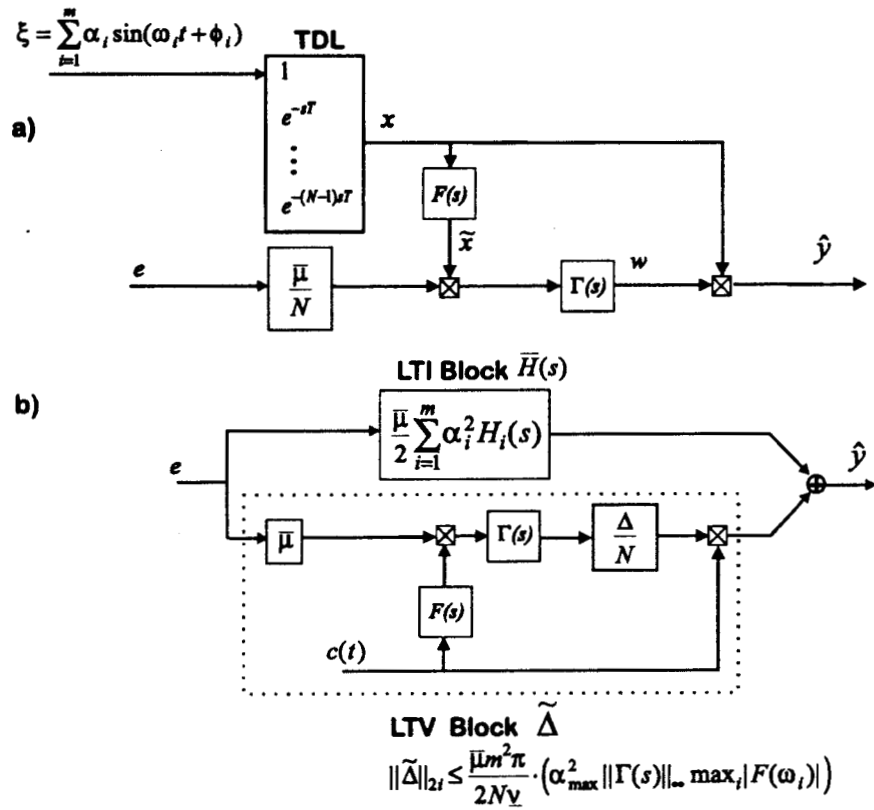


Figure 3.2: LTI/LTV decomposition of \mathcal{H} for harmonic adaptive system with TDL basis

4 Robustness Analysis

The configuration for robustness analysis has been depicted earlier in Figure 2.1. It will be discussed in more detail below.

4.1 Plant Model

Let the plant $P(s)$ be given as,

$$P(s) = \hat{P}(s)(1 + W_M(s)\Delta_M(s)) \quad (4.22)$$

where $\hat{P}(s)$ is a specified nominal transfer function, and Δ_M denotes a norm-bounded multiplicative plant uncertainty,

$$\|\Delta_M(s)\|_\infty \leq 1 \quad (4.23)$$

4.2 Controller Model

By the LTI/LTV decomposition, the adaptive controller can be written as,

$$\mathcal{H}: \hat{y} = \bar{H}(p)e + \tilde{\Delta}[e] \quad (4.24)$$

Here, $\bar{H}(s)$ is the LTI block given in (3.10), and the $\tilde{\Delta}$ is the LTV block. The LTV block can be further decomposed as,

$$\tilde{\Delta} = W_A \Delta_A \quad (4.25)$$

where W_A is a scalar *constant* given by the RHS of (3.12), and Δ_A is an LTV operator whose induced 2-norm is bounded by unity, i.e.,

$$\|\Delta_A\|_{2i} \leq 1 \quad (4.26)$$

4.3 Nominal Stability

Setting $\Delta_M = \Delta_A = 0$ the characteristic equation of the closed-loop system shown in Figure 2.1 is given by,

$$1 + \bar{H}(s)\hat{P}(s) = 0 \quad (4.27)$$

The nominal system is internally stable if $\hat{P}(s)$ and $\bar{H}(s)$ are both stable separately, and the roots of the characteristic equation (4.27) are in the open LHP [10].

4.4 Nominal Performance

Setting $\Delta_M = \Delta_A = 0$, the closed-loop transfer function from the noise input y to the output error e is given by,

$$G_{ey}(s) = \frac{\hat{P}(s)}{1 + \bar{H}(s)\hat{P}(s)} \quad (4.28)$$

Due to the form of the adaptive control $\bar{H}(s)$ given in (3.9),(3.10), there will be notches in this transfer function in the vicinity of the disturbance tone frequencies. The depth of these notches indicates performance in terms of disturbance attenuation.

4.5 Robust Stability

For analysis of robust stability, the adaptive system shown in Figure 2.1 is put into standard $M - \Delta$ form,

$$\begin{bmatrix} y_1(s) \\ y_2(s) \end{bmatrix} = M(s) \cdot \begin{bmatrix} u_1(s) \\ u_2(s) \end{bmatrix} \quad (4.29)$$

$$M(s) = \frac{1}{1 + \bar{H}(s)\hat{P}(s)} \cdot \begin{bmatrix} -W_M\hat{P}(s)\bar{H}(s) & -W_M\hat{P}(s) \\ W_A & -W_A\hat{P}(s) \end{bmatrix} \quad (4.30)$$

$$\Delta = \begin{bmatrix} \Delta_M & 0 \\ 0 & \Delta_A \end{bmatrix} \quad (4.31)$$

Assume that nominal stability is satisfied. Then using the small gain theorem [6][14] and the fact that $\|\Delta\|_{2i} \leq 1$, a sufficient condition for robust L_2 stability is given by,

$$\|M(j\omega)\|_\infty < 1 \quad (4.32)$$

This is equivalent to the condition,

$$\bar{\sigma}(M(j\omega)) < 1 \text{ for all } \omega \quad (4.33)$$

This test involves the maximum singular value of M at each frequency. However, because the uncertainty in (4.31) is structured with two blocks, a less conservative sufficient condition for robust stability is given as,

$$\mu_s(M(j\omega)) < 1 \text{ for all } \omega \quad (4.34)$$

where μ_s denotes the *structured singular value* computed with respect to the 2x2 diagonal matrix Δ given in (4.31) (cf., [7]).

Unfortunately, since the operator Δ_A is LTV, standard μ theory does not strictly apply. However, it is shown in Appendix A that for the present application, (4.34) can still be interpreted as a sufficient condition for robust stability in the weaker sense of L_2 .

5 Case Study

The robustness analysis described above can be applied to a wide variety of adaptive algorithms and regressor choices. The case study will focus on the commonly used Filtered-X algorithm [15][9][8][5][16] specialized to having a leakage modification and a tap-delay-line regressor.

5.1 Set-Up

Filtered-X Algorithm with Leakage

$$\dot{w} = \sigma w + \mu \tilde{x}(t)e(t) \quad (5.1)$$

$$\tilde{x} = F(p)x(t) \quad (5.2)$$

$$\hat{y} = w^T x \quad (5.3)$$

TDL Regressor

$$x = [x_1, \dots, x_N]^T \in R^N \quad (5.4)$$

$$x_\ell = e^{-(\ell-1)pT} \xi, \quad \ell = 1, \dots, N \quad (5.5)$$

$$\xi(t) = \sum_{i=1}^2 \alpha_i \sin(\omega_i t + \phi_i); \quad \alpha_i > 0 \quad (5.6)$$

Applying the LTI/LTV decomposition gives,

LTI Block for TDL Regressor

$$\bar{H}(s) \triangleq \frac{\bar{\mu}}{2} \sum_{i=1}^m \alpha_i^2 \cdot \frac{F_R(i)(s + \sigma) + F_I(i)\omega_i}{s^2 + 2\sigma s + (\sigma^2 + \omega_i^2)} \quad (5.7)$$

$$F_R(i) \triangleq \text{Re}(F(j\omega_i)); \quad F_I(i) \triangleq \text{Im}(F(j\omega_i)) \quad (5.8)$$

Bound on LTV Block for TDL Regressor

$$\|\tilde{\Delta}\|_{2i} \leq \frac{\bar{\mu}m}{N\sigma} \cdot \bar{\sigma}(\Delta) \max_i |F(\omega_i)| \triangleq W_A \quad (5.9)$$

The filter $F(s)$ of the FX algorithm will be chosen equal to the nominal plant model, i.e.,

$$F(s) = \hat{P}(s) \quad (5.10)$$

Plant

$$P(s) = \hat{P}(s)(1 + W_M(s)\Delta_M(s)) \quad (5.11)$$

$$W_M(s) = \frac{2s}{s + c_M} \quad (5.12)$$

$$\|\Delta_M\|_\infty \leq 1 \quad (5.13)$$

$$\hat{P}(s) = \frac{b_p}{s + a_p} - \frac{\ell_p}{s^2 + 2\zeta_p\omega_p s + \omega_p^2} \quad (5.14)$$

$$\ell_p = \omega_p^2 \left| \frac{b_p}{j\omega_p + a_p} \right| \quad (5.15)$$

$$a_p = b_p = 2\pi(20); \zeta_p = .1; \omega_p = 2\pi(30) \quad c_M = 2\pi(50) \quad (5.16)$$

The nominal plant transfer function is shown in Figure 5.1, and the multiplicative uncertainty is shown in Figure 5.2.

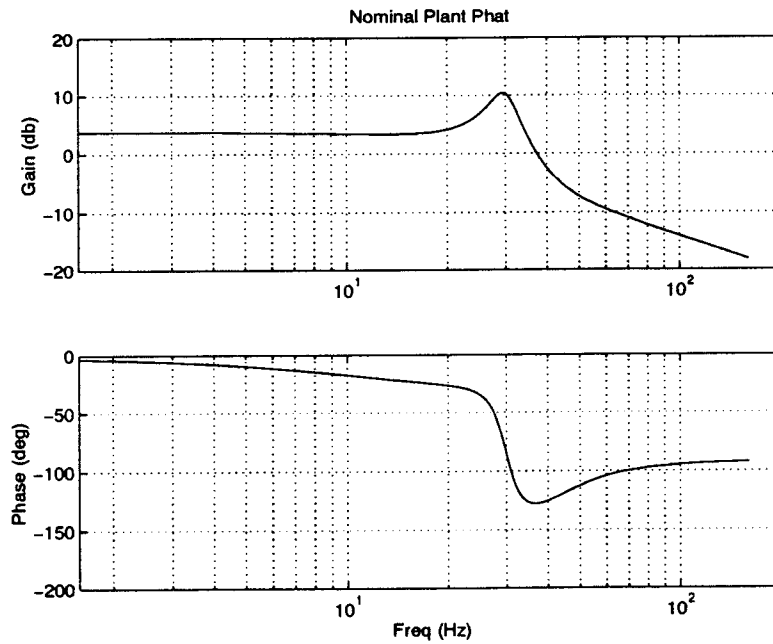


Figure 5.1: Nominal plant \hat{P}

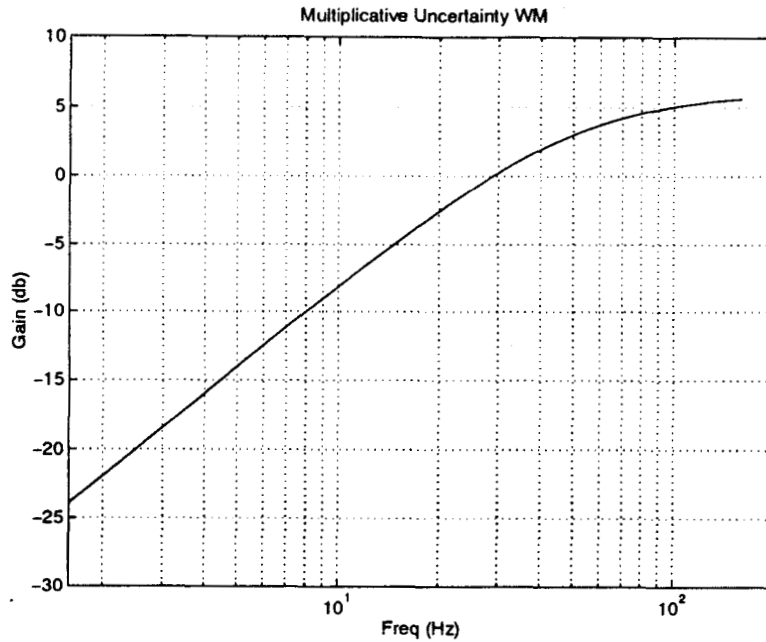


Figure 5.2: Multiplicative uncertainty $W_M(s)$

5.2 Case Study 1

Parameter values are chosen as follows: $\omega_1 = 2\pi(12)$, $\omega_2 = 2\pi(24)$, $\alpha_1 = \alpha_2 = 1$, $\bar{\mu} = 20$, $\sigma = .001$, $T = .01$; $N = 50$.

The controller additive uncertainty can be calculated with the aid of formula (3.12) to give,

$$W_A = 2.4e - 11 \quad (5.17)$$

One of the main reasons that (5.17) is so small is that, as shown in Figure 5.3, there are deep minima of $\bar{\sigma}(\Delta)/N$ at particular choices of N . The choice $N = 50$ used here is exactly at a minimum, and such a choice in practice would require prior knowledge of the disturbance frequencies. The use of such minimizing values of N and T for systematic design purposes was first advocated in Elliott et. al. [8].

In the more practical case where the disturbances are unknown, and N is not in a local minimum, then N will generally have to be chosen significantly larger to ensure that $\bar{\sigma}(\Delta)/N$ remains small. This situation will be treated in more detail in Case 2.

The LTI block $\bar{H}(s)$ of the adaptive controller is shown in Figure 5.4. The large gains at the disturbance frequencies are clearly discernable. The nominal loop gain $\bar{H}(s)\hat{P}(s)$ is shown as a Nyquist plot in Figure 5.5 and (blown up) in Figure 5.6, and as a Bode plot in Figure 5.7.

It can be verified from either the root locations or the Nyquist plot that the nominal

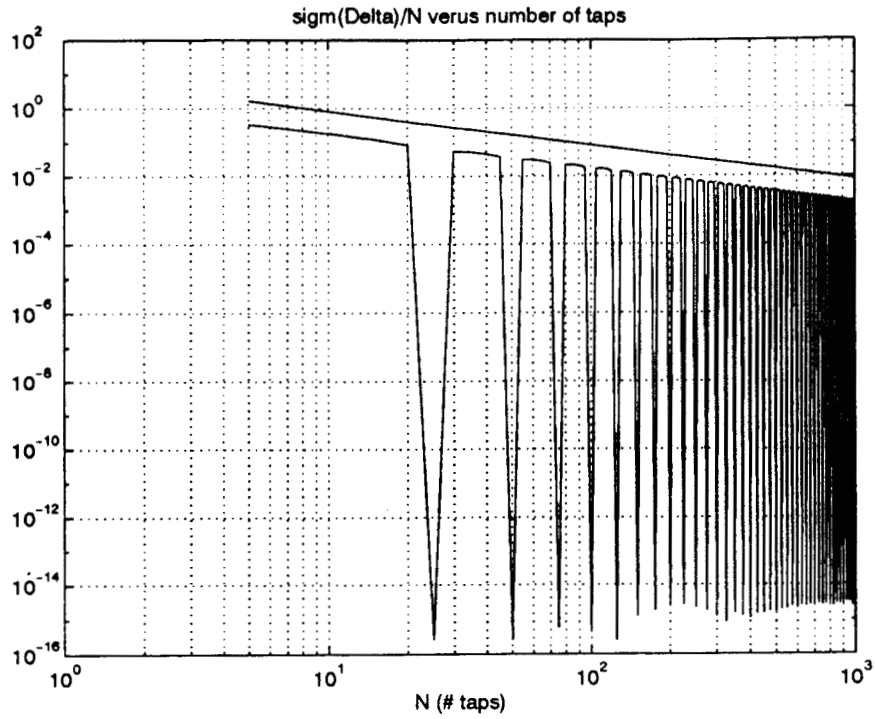


Figure 5.3: Case 1: $\bar{\sigma}(\Delta)/N$ versus N

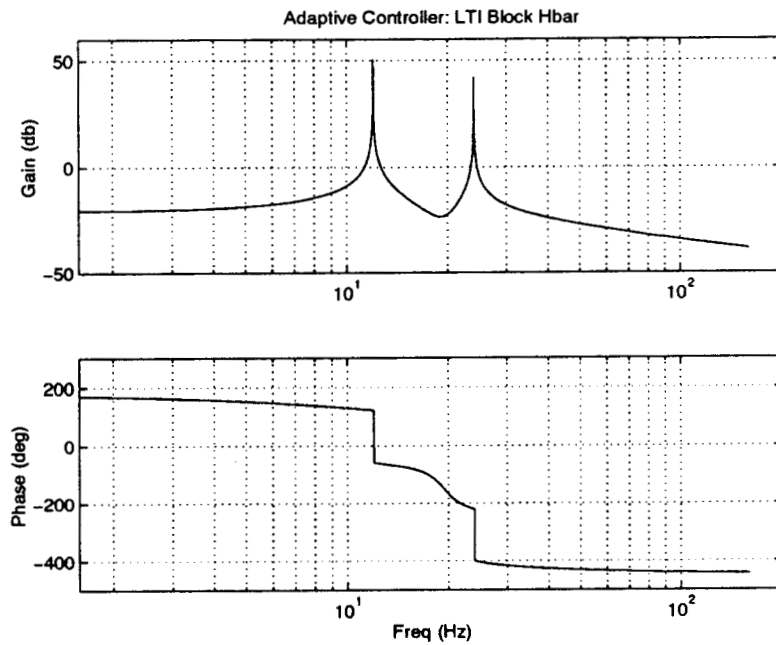


Figure 5.4: Case 1: LTI block $\bar{H}(s)$ of adaptive controller

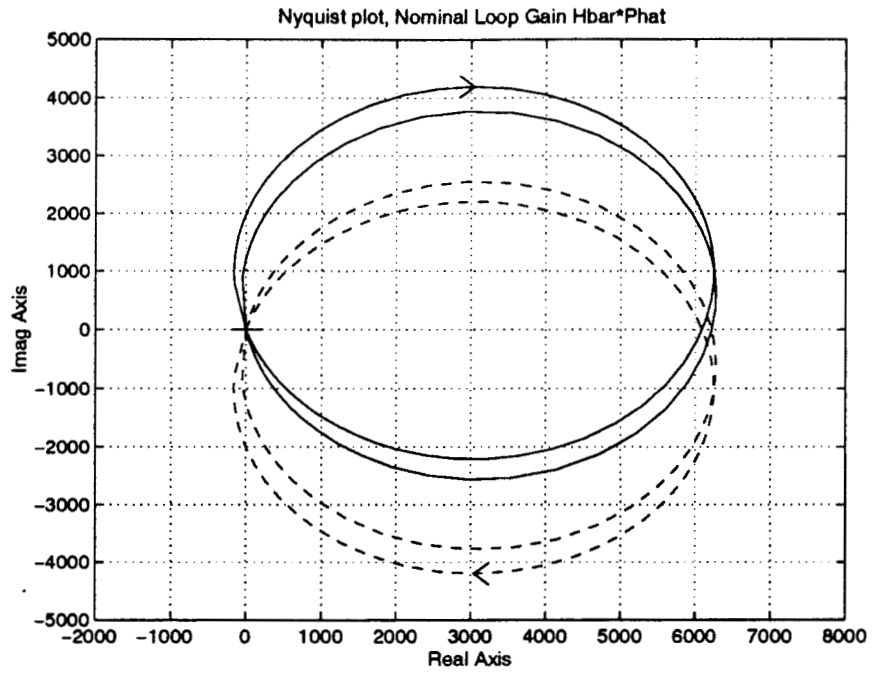


Figure 5.5: Case 1: Nyquist plot of nominal loop gain $\bar{H}(s)\hat{P}(s)$

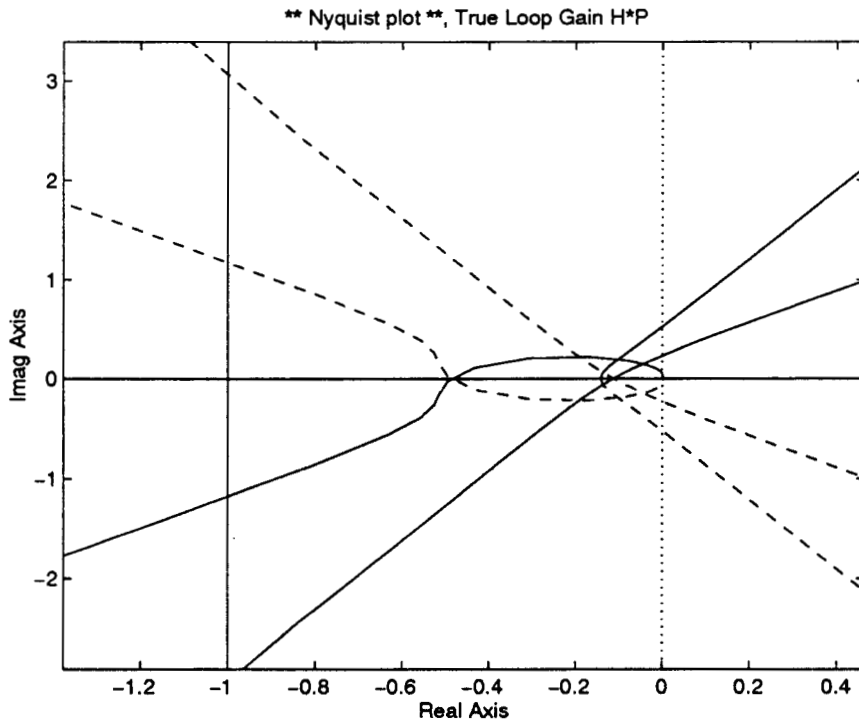


Figure 5.6: Case 1: Nyquist plot (blow up) of nominal loop gain $\bar{H}(s)\hat{P}(s)$

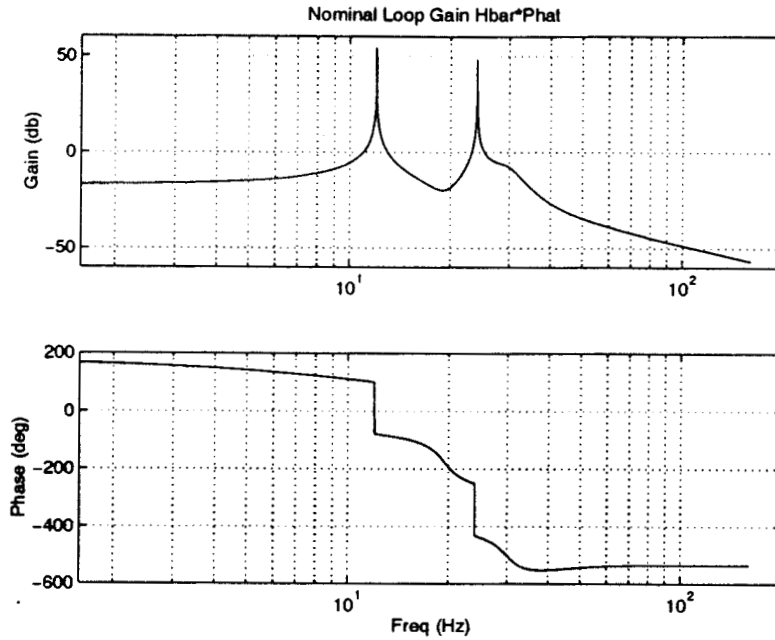


Figure 5.7: Case 1: Bode plot of nominal loop gain $\bar{H}(s)\hat{P}(s)$

system is stable. The nominal performance is plotted in Figure 5.8 as the transfer function $G(s)_{ey}$ from disturbances y to the plant output e . The steep notches indicate an impressive 40 – 50 db of attenuation for both disturbance tones.

The structured singular value is plotted in Figure 5.9. It is less than unity demonstrating that the adaptive system in this case is stable.

5.3 Case Study 2

As shown in Figure 5.3 the choice of $N = 50$ in Case 1 was very fortuitous in giving a small W_A . It is deduced from the relation shown in Figure 5.3, that N would have to be upwards of 5,000,000 to give the same W_A if one did not have sufficient a-priori information about the disturbance frequencies to choose N at a local minimum. Clearly, this is too large a number of taps to implement in practice.

One can try to offset needing such a large N by lowering W_A in other ways. For this case study, the value of σ is increased two orders of magnitude for this purpose. These two orders of magnitude effectively reduce the requirement on N from 5,000,000 to 50,000.

The actual number used will be $N = 50,010$ to make the problem challenging by ensuring that we are not at a local minimum. This is still quite large, and underscores the need for better basis functions than TDLs for this class of problems. Parameters for the present Case 2 are the same as Case 1 except for the choice of N and σ .

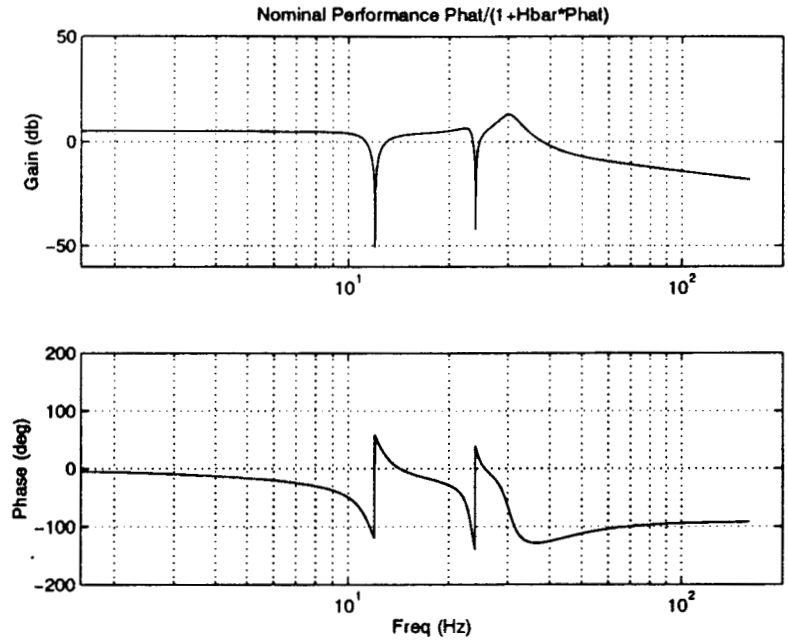


Figure 5.8: Case 1: Performance transfer function $G(s)_{ey}$

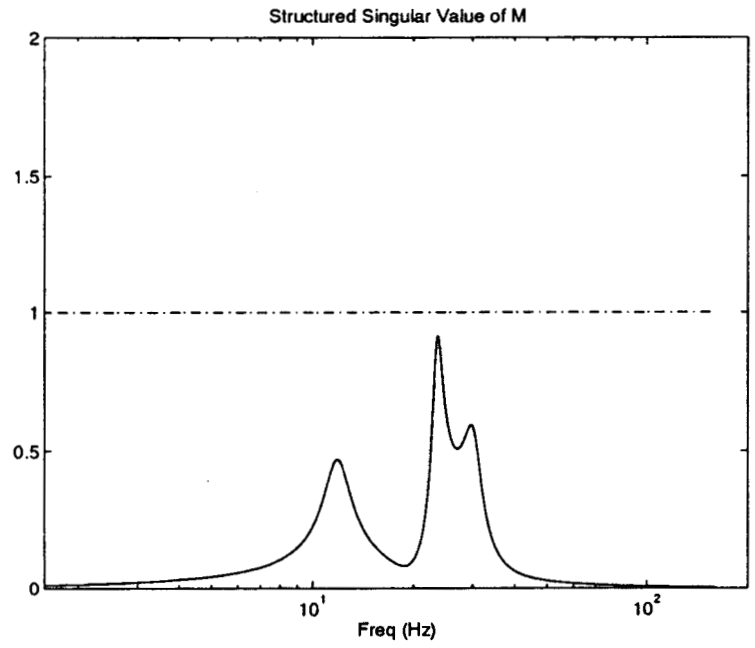


Figure 5.9: Case 1: Structured singular value $\mu(M(s))$

Parameter values are chosen as follows: $\omega_1 = 2\pi(12)$, $\omega_2 = 2\pi(24)$, $\alpha_1 = \alpha_2 = 1$, $\bar{\mu} = 20$, $\sigma = .1$, $T = .01$; $N = 50010$.

The controller additive uncertainty can be calculated with the aid of formula (3.12) to give,

$$W_A = .033357 \quad (5.18)$$

The adaptive controller $\bar{H}(s)$ is shown in Figure 5.10. The nominal loop gain $\bar{H}(s)\hat{P}(s)$ is shown as a Nyquist plot in Figure 5.11 and (blown up) in Figure 5.12, and as a Bode plot in Figure 5.13.

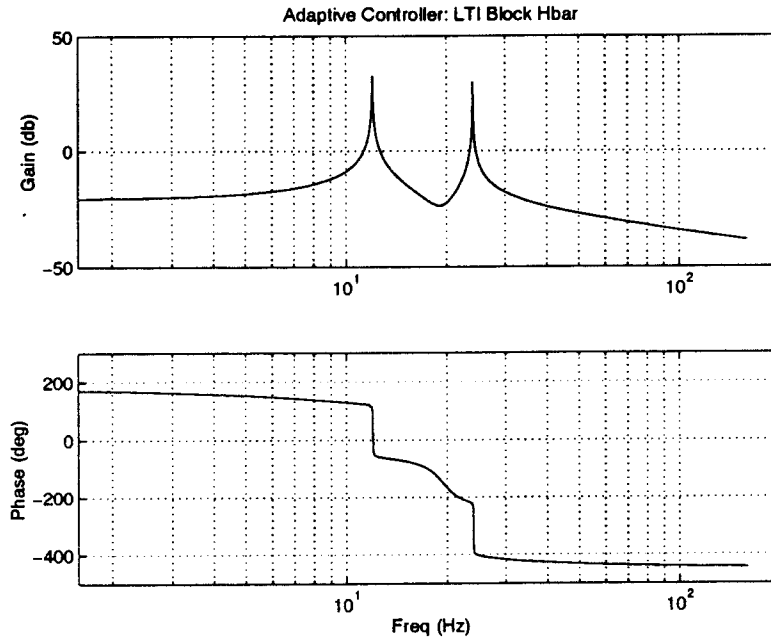


Figure 5.10: Case 2: LTI block $\bar{H}(s)$ of adaptive controller

It can be verified from either the root locations or the Nyquist plot that the nominal system is stable. The nominal performance is plotted in Figure 5.14 as the transfer function from disturbance inputs to the plant output. The notches indicate approximately 30 db of attenuation for each of the two disturbance tones. This performance is not as impressive as for Case 1, due predominantly to the increased leakage parameter σ which induces a significantly shallower notch according to (5.7).

The structured singular value is plotted in Figure 5.15. It is less than unity demonstrating that the adaptive system in this case is stable.

In summary, when N and T are chosen without prior knowledge of the disturbance tones, the value for W_A can be quite large. Case Study 2 demonstrates the use of leakage to decrease the size of W_A , rather than requiring an unrealistically large number of taps. The number of taps required, however, is still large and indicates the need for a better

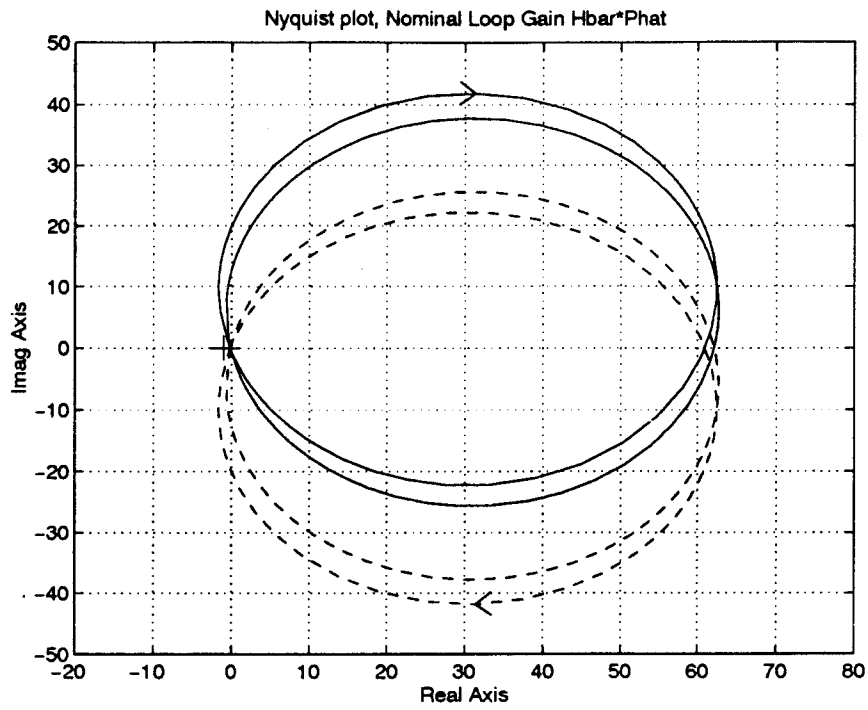


Figure 5.11: Case 2: Nyquist plot of nominal loop gain $\bar{H}(s)\hat{P}(s)$

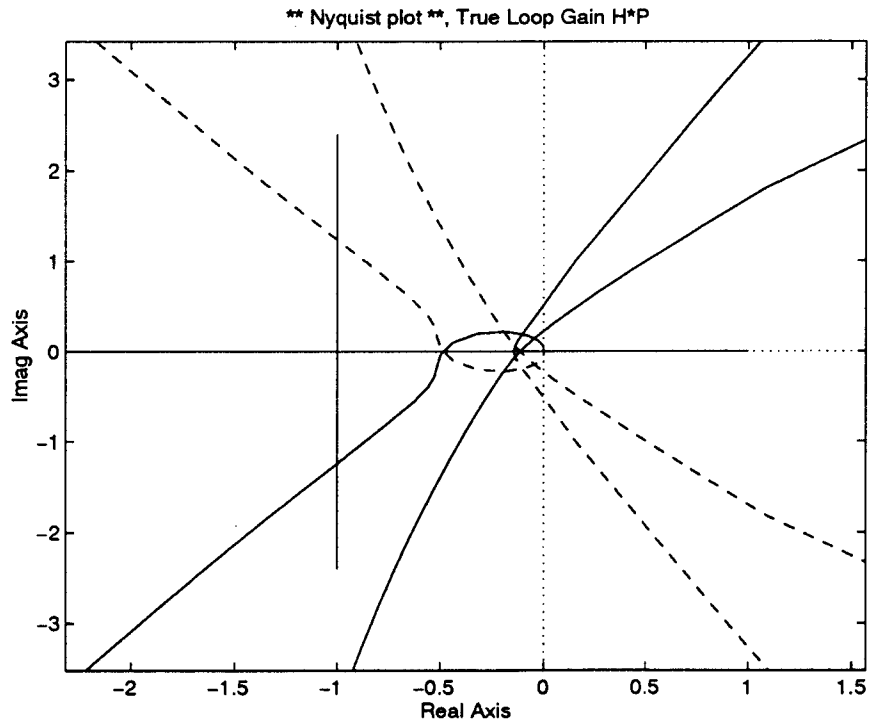


Figure 5.12: Case 2: Nyquist plot (blow up) of nominal loop gain $\bar{H}(s)\hat{P}(s)$

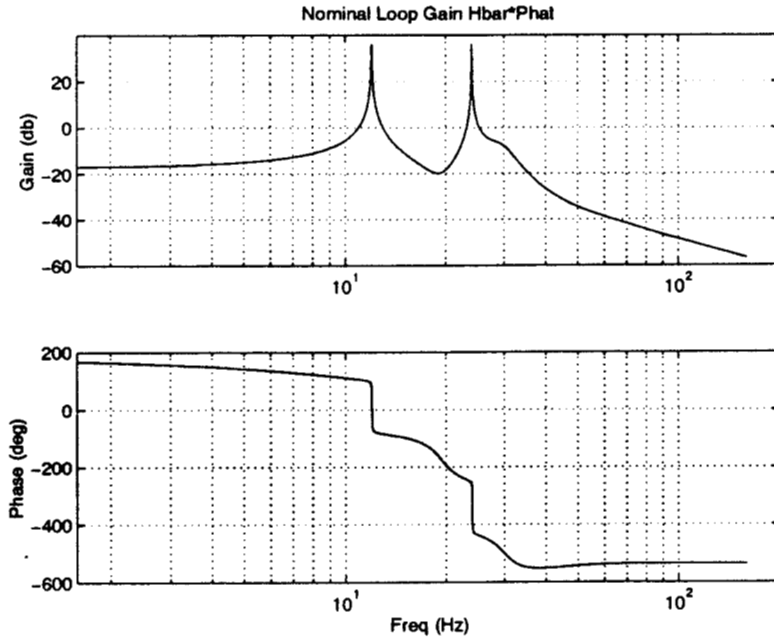


Figure 5.13: Case 2: Bode plot of nominal loop gain $\bar{H}(s)\hat{P}(s)$

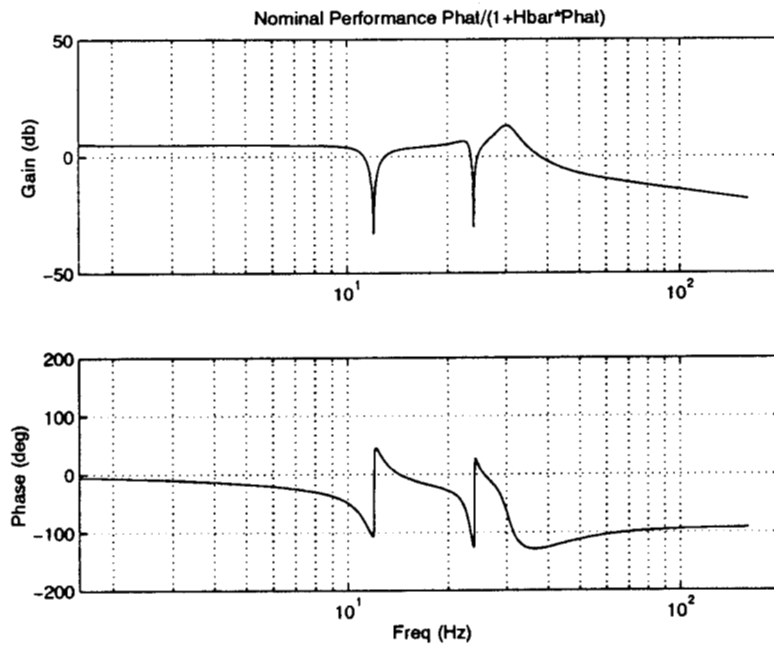


Figure 5.14: Case 2: Performance transfer function $G(s)_{ey}$

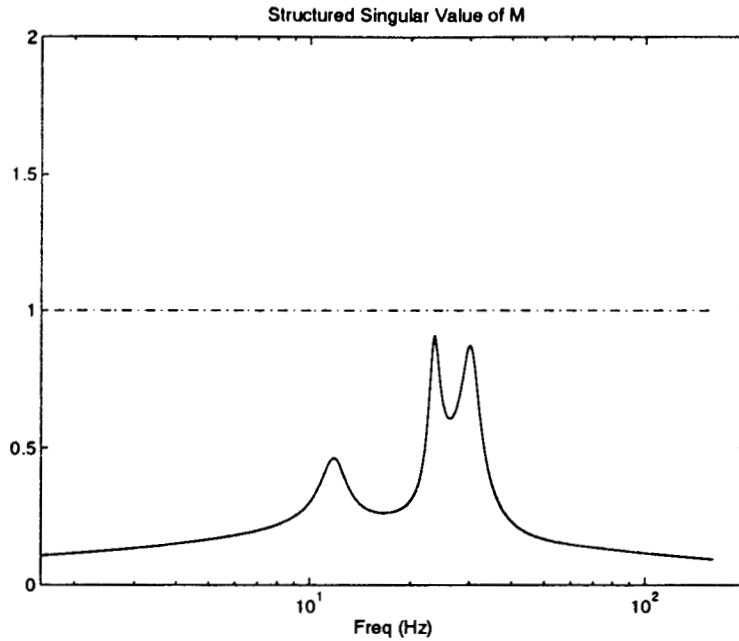


Figure 5.15: Case 2: Structured singular value $\mu(M(s))$

regressor basis than using a TDL.

5.4 Case Study 3

This case extends Case 2 by showing what happens when the disturbances are shifted to higher frequencies into a region where there is more plant uncertainty. Specifically, the disturbance tones are now taken as,

$$\omega_1 = 2\pi(13); \omega_2 = 2\pi(28) \quad (5.19)$$

As seen from Figure 5.2, the 28 Hertz tone is starting to impinge on the region where the multiplicative uncertainty is unity.

Parameter values are chosen as follows: $\omega_1 = 2\pi(13)$, $\omega_2 = 2\pi(28)$, $\alpha_1 = \alpha_2 = 1$, $\bar{\mu} = 20$, $\sigma = .1$, $T = .01$; $N = 50010$.

The controller additive uncertainty can be calculated with the aid of formula (3.12) to give,

$$W_A = .020896 \quad (5.20)$$

The adaptive controller $\bar{H}(s)$ is shown in Figure 5.16. The nominal loop gain $\bar{H}(s)\hat{P}(s)$ is shown as a Nyquist plot in Figure 5.17 and (blown up) in Figure 5.18, and as a Bode plot in Figure 5.19.

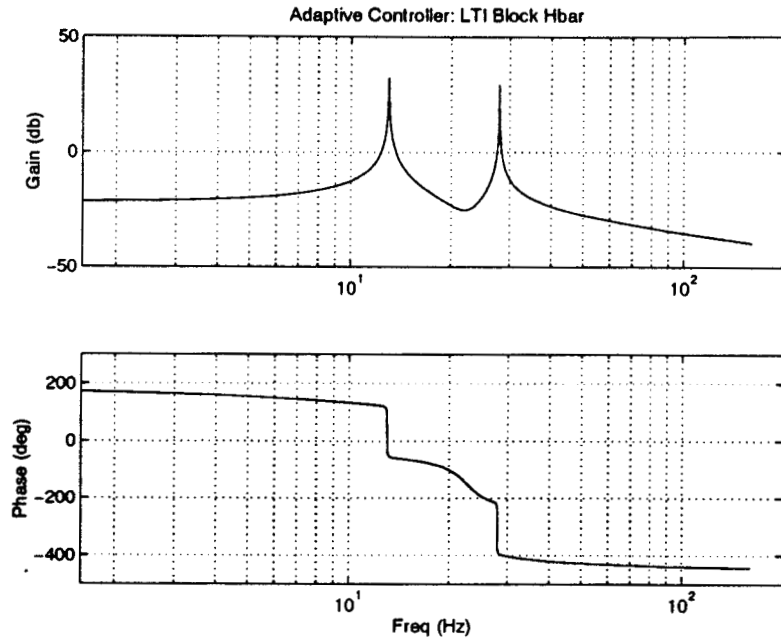


Figure 5.16: Case 3: LTI block $\bar{H}(s)$ of adaptive controller

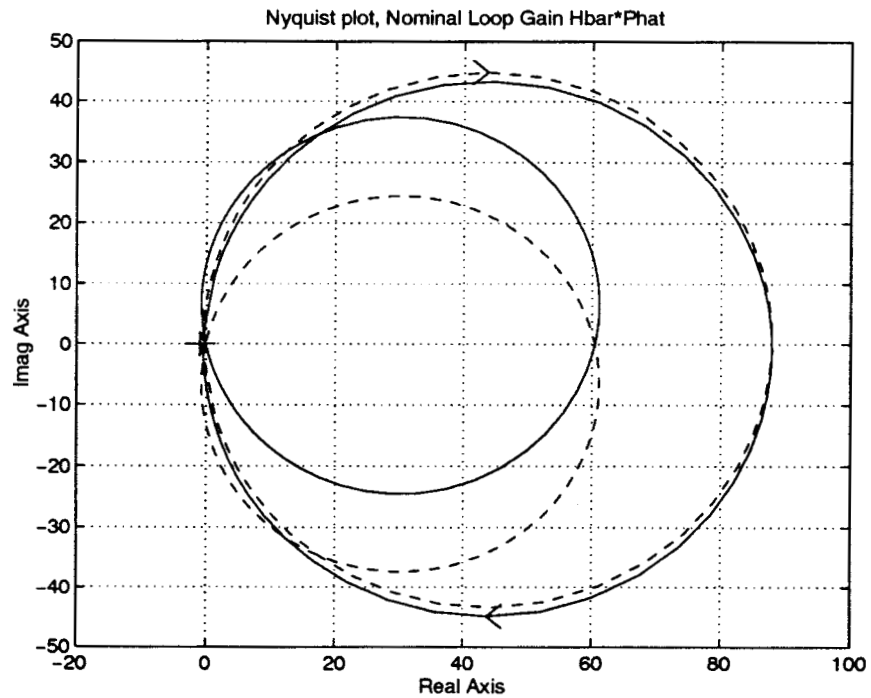


Figure 5.17: Case 3: Nyquist plot of nominal loop gain $\bar{H}(s)\hat{P}(s)$

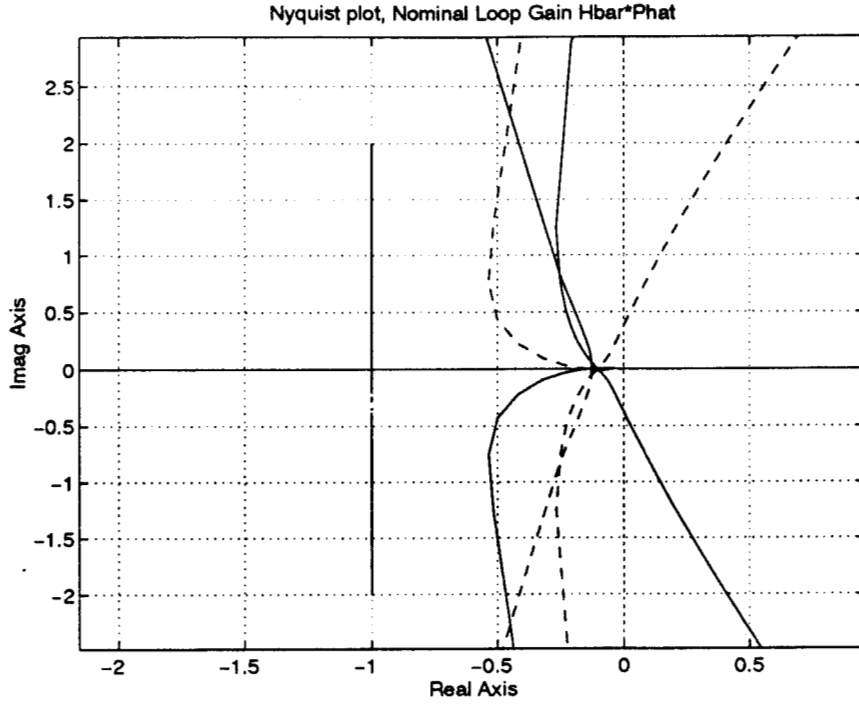


Figure 5.18: Case 3: Nyquist plot (blow up) of nominal loop gain $\bar{H}(s)\hat{P}(s)$

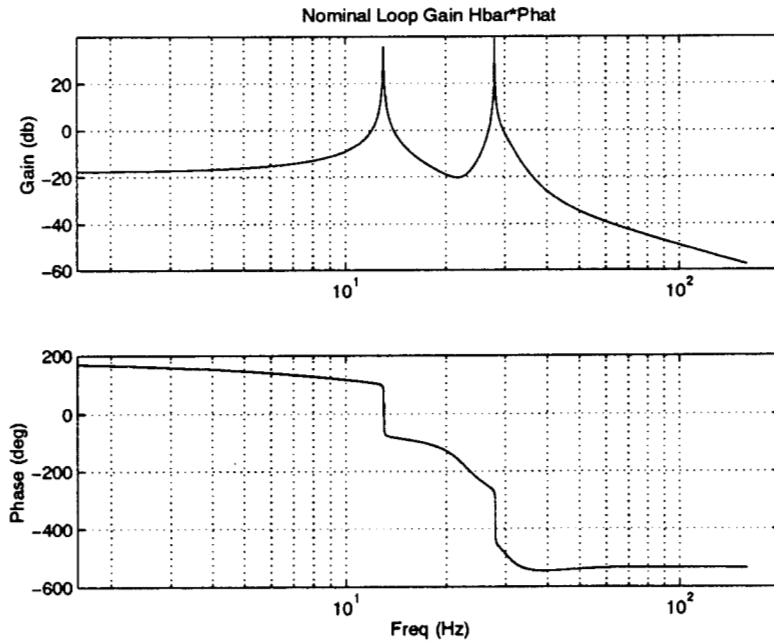


Figure 5.19: Case 3: Bode plot of nominal loop gain $\bar{H}(s)\hat{P}(s)$

It can be verified from either the root locations or the Nyquist plot that the nominal system is stable. The nominal performance is plotted in Figure 5.20 as the transfer function from disturbance inputs to the plant output. The notches indicate approximately 30 db of attenuation for both disturbance tones, similar to Case 2.

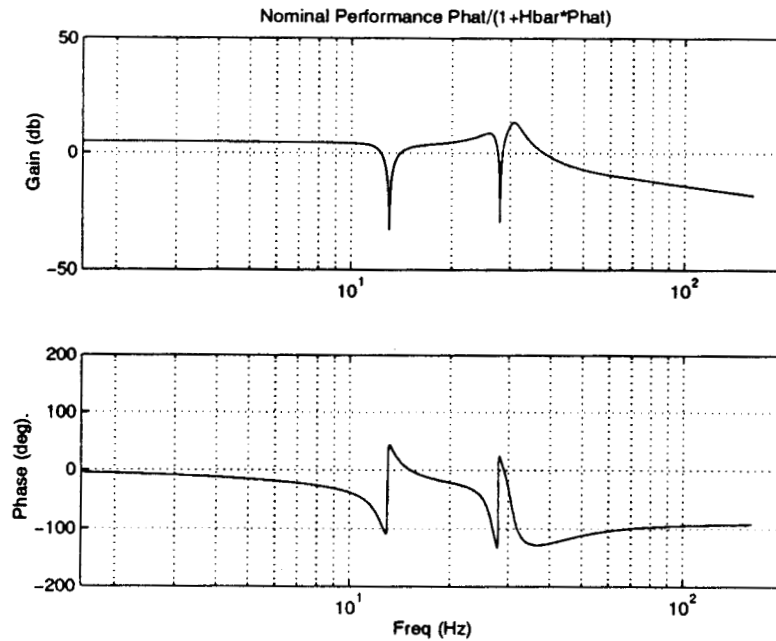


Figure 5.20: Case 3: Performance transfer function $G(s)_{ey}$

The structured singular value is plotted in Figure 5.21. It is seen that it becomes larger than unity in the vicinity of the 28 Hertz disturbance tone. Since the μ condition (4.34) is only sufficient, it cannot be concluded that the system will be unstable. However, consider the specific perturbation,

$$W_M \Delta_M = \frac{-2s}{s + c_M} \quad (5.21)$$

which can be shown to satisfy the multiplicative bound (5.12), and in addition let $\Delta_A = 0$. With this choice, the actual loop gain is shown in the Nyquist plot Figure 5.22, and blown up in Figure 5.23. The encirclement of the critical point indicates that the system is indeed unstable under this class of perturbations.

In summary, Case Study 3 demonstrates that there may be a need to prefilter the signal ξ to avoid cancelling disturbance tones in regions of large plant uncertainty.

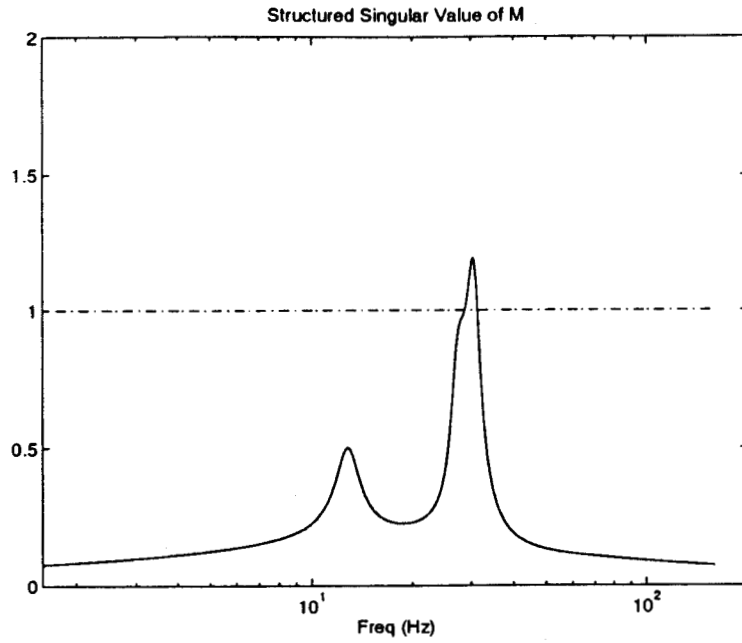


Figure 5.21: Case 3: Structured singular value $\mu(M(s))$

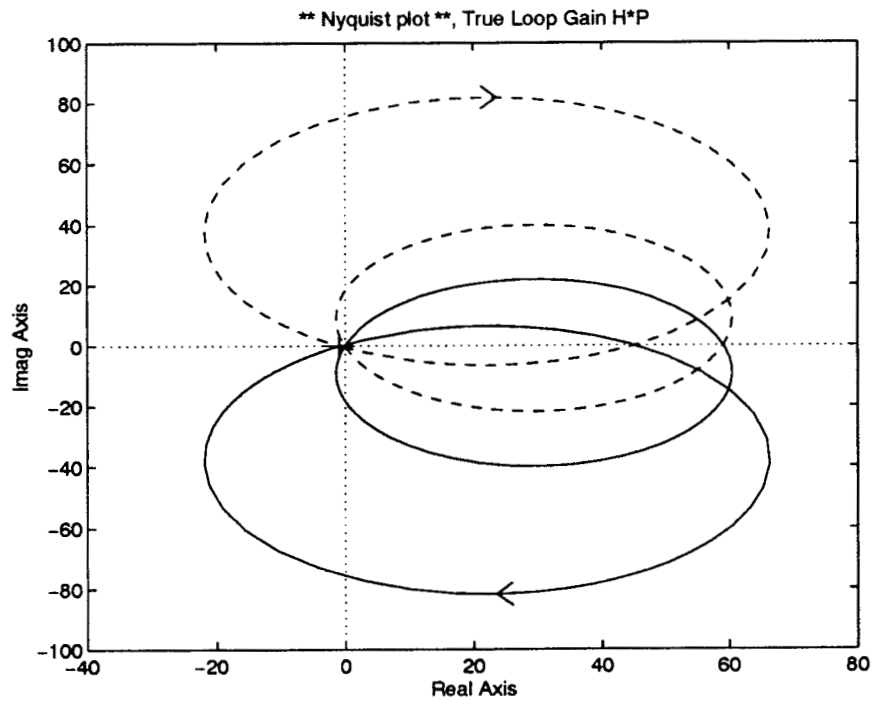


Figure 5.22: Case 3: Nyquist plot of actual loop gain $\bar{H}(s)P(s)$

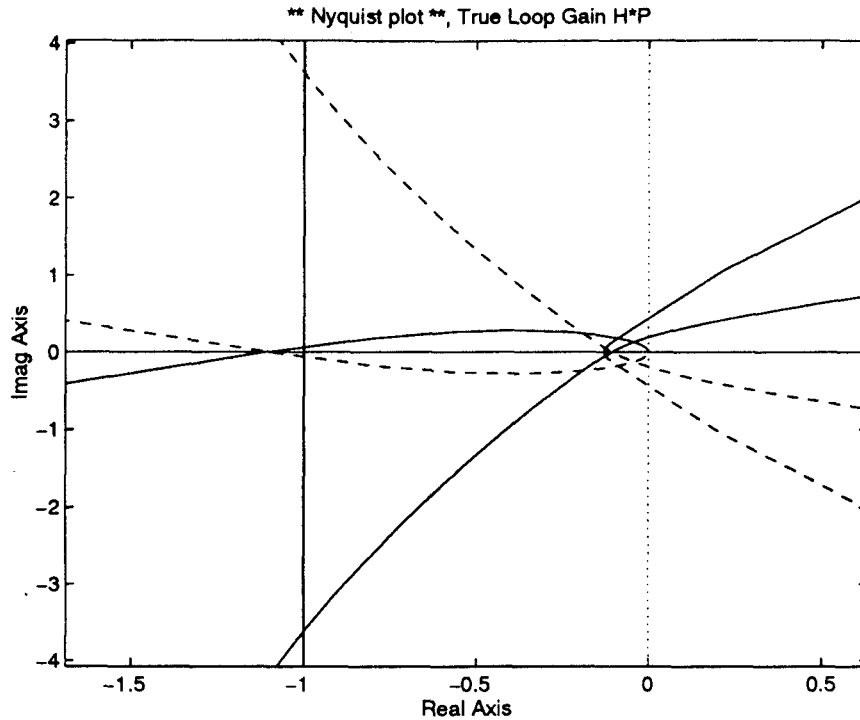


Figure 5.23: Case 3: Nyquist plot (blow up) of actual loop gain $\overline{H}(s)P(s)$

6 Conclusions

Using a recently developed LTI/LTV decomposition, a robust control theory framework was developed to analyze a class of adaptive feedforward algorithms for cancelling sinusoidal noise. Sufficient conditions for robust stability in L_2 were established in terms of the structured singular value. A case study was presented, analyzing adaptive noise cancellation in the presence of a plant resonance blocking the noise cancellation path. The analysis allowed for a nonminimum-phase resonance in the plant, a multiplicative error in the plant description, and additive error in the control model corresponding to using an overparametrized regressor. The case study gave significant insight into several properties of nominal performance and robust stability.

A potential drawback to using the method in practice is that a separate mu analysis must be performed for each combination of disturbance tone amplitude and frequency value, i.e., $\alpha_i, \omega_i, i = 1, \dots, m$. This can lead to a large combinatorial problem. However, out of fairness, it is important to realize that this difficulty is intrinsic to the problem at hand rather than any method used to analyze it. The expressions for $\overline{H}(s)$ and W_A (and hence stability properties), are dependent on the disturbance amplitudes and frequencies. Any stability test which does not explicitly take these into account, cannot properly discriminate stable from unstable configurations.

Fruitful areas for future investigation include simplifying the mu tests, examining robust performance properties, and finding improved basis functions which converge faster than $1/N$ to the XO condition.

Acknowledgements

This research was performed at the Jet Propulsion Laboratory, California Institute of Technology, under contract with the National Aeronautics and Space Administration.

A Appendix: Mu for Mixed LTI/LTV Uncertainty

This appendix is included to show that for the block diagram in Figure 2.1 having a single LTV perturbation Δ_A , and a single LTI perturbation Δ_M , the mu condition (4.34) is a sufficient condition for robust stability in sense of L_2 . This appendix represents a simplification of existing results on LTV perturbations found in Shamma [13], Poolla and Tikku [12] and Packard [11], and no claim is made to originality. It is included only to make the paper more readable and self-contained.

The perturbation operator,

$$\Delta = \begin{bmatrix} \Delta_M(s) & 0 \\ 0 & \Delta_A \end{bmatrix} \quad (\text{A.1})$$

is identical to a rescaled perturbation operator,

$$\Delta = \mathcal{D}^{-1} \Delta \mathcal{D} \quad (\text{A.2})$$

where,

$$\mathcal{D} = \begin{bmatrix} d_1(s) & 0 \\ 0 & d_2 \end{bmatrix} \quad (\text{A.3})$$

since $d_1(s)$ is an LTI transfer function which commutes with the LTI operator Δ_M , and d_2 is a scalar constant which commutes with the LTV operator Δ_A .

Using (A.2), the equivalent small-gain condition on M for robust L_2 stability can be calculated as,

$$\|\mathcal{D}M\mathcal{D}^{-1}\|_\infty < 1 \quad (\text{A.4})$$

or in terms of maximum singular values,

$$\sup_\omega \bar{\sigma}(\mathcal{D}M(j\omega)\mathcal{D}^{-1}) < 1 \quad (\text{A.5})$$

Since condition (A.5) is sufficient for any choice of \mathcal{D} , it can be made less conservative by optimizing over \mathcal{D} as follows,

$$\min_{d_1(j\omega), d_2} \sup_\omega \bar{\sigma}(\mathcal{D}M(j\omega)\mathcal{D}^{-1}) < 1 \quad (\text{A.6})$$

Here, it is emphasized that the optimization is constrained so that d_2 is a scalar constant.

However, (A.6) is equivalent to the more general *unconstrained* optimization problem,

$$\min_{d_1(j\omega), d_2(j\omega)} \sup_{\omega} \bar{\sigma}(\mathcal{D}(j\omega)M(j\omega)\mathcal{D}^{-1}(j\omega)) < 1 \quad (\text{A.7})$$

where $d_2(s)$ is now treated as a full LTI transfer function, to be optimized over along with $d_1(j\omega)$. Although not at first obvious, the equivalence of (A.7) and (A.6) can be seen by reparametrizing d_1, d_2 as follows,

$$d_1 = \alpha(j\omega); \quad d_2 = \alpha(j\omega)\beta(j\omega) \quad (\text{A.8})$$

for some $\alpha(j\omega) > 0$, and $\beta(j\omega) > 0$. Substituting (A.8) into (A.7) and expanding gives,

$$\mathcal{D}(j\omega)M(j\omega)\mathcal{D}^{-1}(j\omega) = \begin{bmatrix} m_{11}(j\omega) & \frac{1}{\beta(j\omega)} \cdot m_{12}(j\omega) \\ \beta(j\omega) \cdot m_{21}(j\omega) & m_{22}(j\omega) \end{bmatrix} \quad (\text{A.9})$$

It is emphasized that the RHS of (A.9) is not a function of $\alpha(j\omega)$ and hence not a function of $d_2(j\omega)$. Accordingly, d_2 can be arbitrarily assigned (for example as the constant $d_2 = 1$) without changing the outcome of the optimization.

At this point it is noted that Δ for the present application only involves 2 blocks. For 2 blocks, the standard mu measure μ_s is known to be equivalent to [10],

$$\mu_s(M(j\omega)) = \min_{d_1(j\omega), d_2(j\omega)} \bar{\sigma}(\mathcal{D}(j\omega)M(j\omega)\mathcal{D}^{-1}(j\omega)) \quad (\text{A.10})$$

Accordingly, the robust L_2 stability conditions (A.7) can be written equivalently in terms of the mu measure (A.10) as follows,

$$\mu_s(M(j\omega)) < 1 \quad \text{for all } \omega \quad (\text{A.11})$$

In summary, even though mu theory is not strictly applicable to LTV perturbations, when one applies the small gain theorem to this application (a 2-block problem with a single LTV perturbation) one arrives at the mu condition (A.11) as a sufficient condition to ensure robust L_2 stability. The main practical point of this derivation is that standard software for calculating μ can now be applied.

The necessity of condition (A.11) is more subtle and requires the notion of the rate-of-variation of the LTV operator. For more details the reader is referred to [13][12].

The above derivation is also valid for 3 uncertainty blocks with one being LTV and two being LTI. Hence the mu condition (A.11) can still be used for studying adaptive feedforward systems when an additional uncertainty block is added. The additional block can be very handy, being used to model actuator/sensor uncertainties, or any other LTI perturbations occurring in the adaptive loop.

With four or more uncertainty blocks (i.e., assuming only one is LTV), the mu condition (A.11) is no longer sufficient, and the more general unconstrained optimization (A.7) must be solved. This optimization problem is easier to compute than mu, and in fact is often used as an approximation (i.e., strictly speaking an overbound) to μ in practice [10].

References

- [1] D.S. Bayard, *A General Theory of Linear Time Invariant Adaptive Feedforward Systems with Harmonic Regressors*. Jet Propulsion Laboratory, Internal Document JPL D-13556, April 12, 1996.
- [2] D.S. Bayard, "Necessary and sufficient conditions for LTI representations of adaptive systems with sinusoidal regressors," Proc. American Control Conference, Albuquerque NM, June 1997.
- [3] D.S. Bayard, "An LTI/LTV decomposition of adaptive feedforward systems with sinusoidal regressors," Proc. American Control Conference, pp. 2542-2546, Albuquerque NM, June 1997.
- [4] D.S. Bayard, "LTI representations of adaptive systems with tap delay-line regressors under sinusoidal excitation," Proc. American Control Conference, Albuquerque NM, June 1997.
- [5] J.C. Burgess, "Active sound control in a duct: A computer simulation," J. Acoust. Soc. Amer., vol. 70, pp. 715-726, Sept. 1981.
- [6] C.A. Desoer and M. Vidyasagar, *Feedback Systems: Input-Output Properties*. New York: Academic Press, 1975.
- [7] J.C. Doyle, "Analysis of feedback systems with structured uncertainties," IEE Proc. Part D, vol. 129, pp. 242-250, 1982.
- [8] S.J. Elliott, I.M. Stothers, and P.A. Nelson, "A multiple error LMS algorithm and its application to the active control of sound and vibration," IEEE Trans. Acoustics, Speech and Signal Processing, vol. ASSP-35, no. 10, pp. 1423-1434, October 1987.
- [9] D.R. Morgan, "An analysis of multiple correlation cancellation loops with a filter in the auxiliary path," IEEE Trans. Acoustics, Speech and Signal Proc., vol. 28, no. 4, pp. 454-467, August 1980.
- [10] M. Morari and E. Zafriou, *Robust Process Control*. Englewood Cliffs, NJ: Prentice Hall, 1989.
- [11] A. Packard, "Whats New with μ : Structured Uncertainty in Multivariable Control," Ph.D. Thesis, University of California, Berkeley, 1987.
- [12] K. Poolla and A. Tikku, "Robust performance against time-varying structured perturbations," IEEE Trans. Auto. Contr., vol. 40, no. 9, pp. 1589-1602, September 1995.
- [13] J. Shamma, "Robust stability with time-varying structured uncertainty," IEEE Trans. Auto. Contr., vol. 39, no. 4, pp. 714-724, 1994.

- [14] A. Weinmann, *Uncertain Models and Robust Control*. New York: Springer-Verlag, 1991.
- [15] B. Widrow, "Adaptive filters," in *Aspects of Network and System Theory*, R.E. Kalman and N. De Claris, Eds., New York: Holt Rinehart, Winston 1971.
- [16] B. Widrow, D. Shur, and S. Shaffer, "On adaptive inverse control," in Proc. 15th Asilomar Conf. Circuits, Systems. Computation, pp. 185-189. 1981.